

Disclaimer

This note has not been internally reviewed by the DØ Collaboration. Results or plots contained in this note were only intended for internal documentation by the authors of the note and they are not approved as scientific results by either the authors or the DØ Collaboration. All approved scientific results of the DØ Collaboration have been published as internally reviewed Conference Notes or in peer reviewed journals.

Submitted for the Proceedings of the Workshop on B-Physics at Hadron Accelerators

ELECTRON IDENTIFICATION IN THE D0 DETECTOR

NINA DENISENKO
Fermi National Laboratory
P.O.Box 500, Batavia, Illinois 60510

for the D0 collaboration

ABSTRACT

We present the characteristics of the D0 detector together with the methods applied to identify electrons. The electron identification technique uses calorimeter information together with data from the central tracking detectors. The fine longitudinal and transverse segmentation of the D0 calorimeter enables us to achieve very good pion rejection for electrons above 20 GeV. The D0 calorimeter also provides excellent linearity of response for electrons above 10 GeV. Here we present recent results of studies of energy response for electrons with energy down to 2 GeV and discuss necessary extensions of electron identification algorithms for B-physics studies.

1. INTRODUCTION

The D0 experiment has just completed its first collider run. The physics goals of this run included mostly the high p_t physics: top, electroweak, QCD, new particle searches and B-physics. It was demonstrated that the design aims of D0, excellent calorimetry, good energy resolution for electrons, photons and jets, high efficiency for events of interest were achieved. In addition to that during the first D0 collider run the opportunities to expand the physics menu to low p_t physics were studied. Because of the plans to increase the luminosity of the Fermilab Collider by 1995/96 up to several units of $10^{31} \text{ cm}^{-2} \text{ sec}^{-1}$ and to drop the bunch spacing to 400 ns (it is $3.5 \mu\text{s}$ now) it is planned to upgrade the central tracking system of the D0 detector in order to meet new demands. At the same time the upgraded tracking system will allow D0 to extend its measurement capabilities towards lower p_t . B-physics such as mixing and CP violation in electron channels which makes it necessary to extend the existing electron ID technique to low energies.

Below we present characteristics of the D0 detector systems used for the electron identification. We also discuss trigger efficiencies, offline algorithms and results of simulation studies for electron identification for the upgraded D0 detector.

2. THE D0 DETECTOR

The D0 detector consists of three major systems: the calorimeters, the central tracking system and the muon system.

D0 LIQUID ARGON CALORIMETER

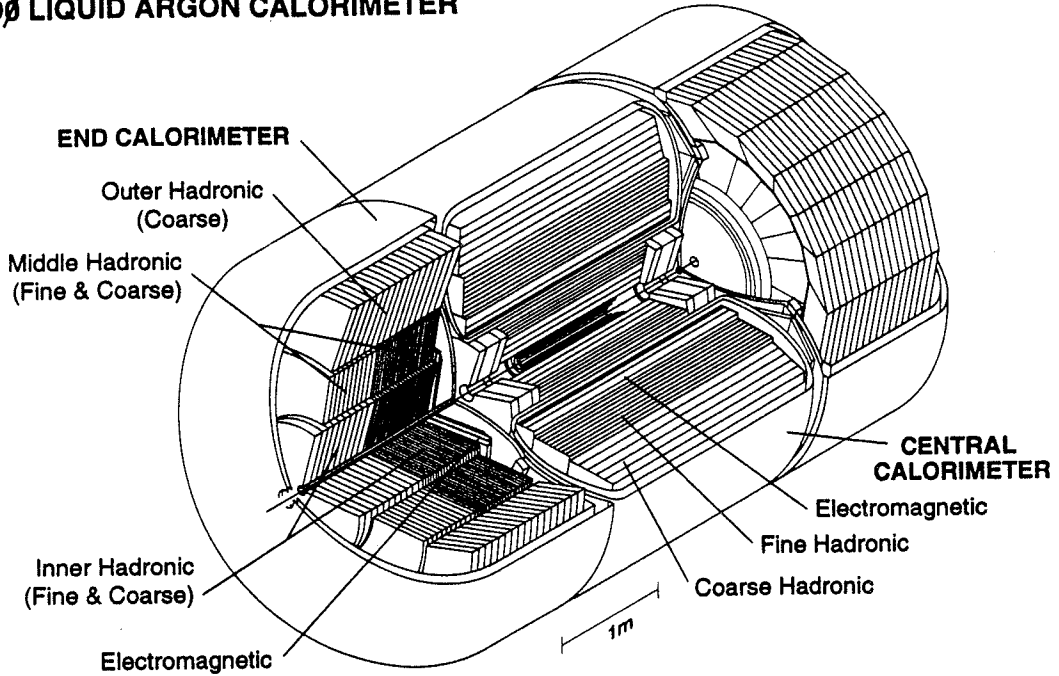


Figure 1. Cutaway view of the D0 calorimeters.

The D0 calorimeters are uranium-liquid argon sampling calorimeters. There are three calorimeters of roughly equal size: a central calorimeter (CC) and two end calorimeters (EC). The cutaway view of the D0 calorimeters is shown in Fig. 1. The end calorimeters each have a ring of 16 outer hadronic modules; inside this is a ring of 16 middle hadronic modules and at the center is a single large inner hadronic module (ECIH). In front of the ECIH is a finely segmented electromagnetic calorimeter (ECEM). The central calorimeter consists a ring of Coarse Hadronic calorimetry, inside of which are the fine hadronic modules followed by the electromagnetic calorimeter (CCEM). The technical details of the calorimeter design can be found in [1,2].

The calorimeters provide full azimuthal ϕ coverage, where ϕ is the angle in the plane perpendicular to the beam. The central calorimeter covers the pseudorapidity region $|\eta| < 1.2$ and the end calorimeters cover $|\eta| > 1.4$ down to the beam pipe ($|\eta| \approx 4.2$). All electromagnetic calorimeter modules are longitudinally segmented into four layers. For the ECEM the longitudinal layers are respectively 0.3, 2.6, 7.9 and 9.3 radiation lengths thick. For the CCEM they are 2, 2, 7 and 10 radiation lengths thick. Transverse segmentation of the calorimeter modules is provided by readout of the calorimeter cells as pseudo-projective towers of size 0.1×0.1 in η and ϕ space. The third longitudinal EM layer typically contains 65% of the electron shower energy and its transverse segmentation is made finer (0.05×0.05). The semiprojective tower geometry for EM modules lines up with fine hadronic modules behind them. The calorimeter modules were tested during several fixed target runs at Fermilab.

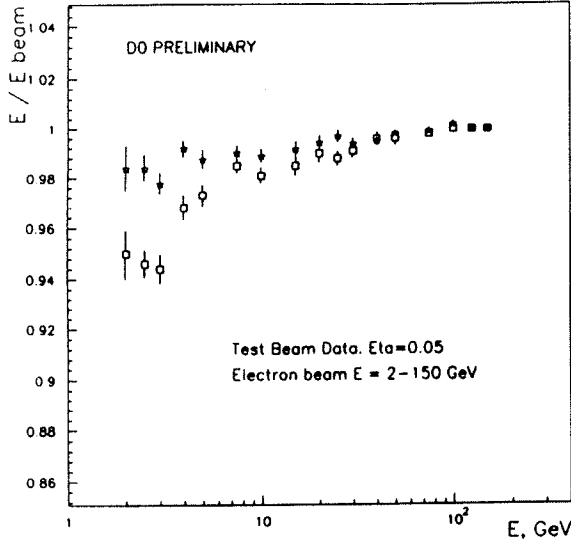


Figure 2. Energy reconstructed in the CC calorimeter normalized to the nominal test beam energy for electrons 2 - 150 GeV for two sets of sampling weights [5].

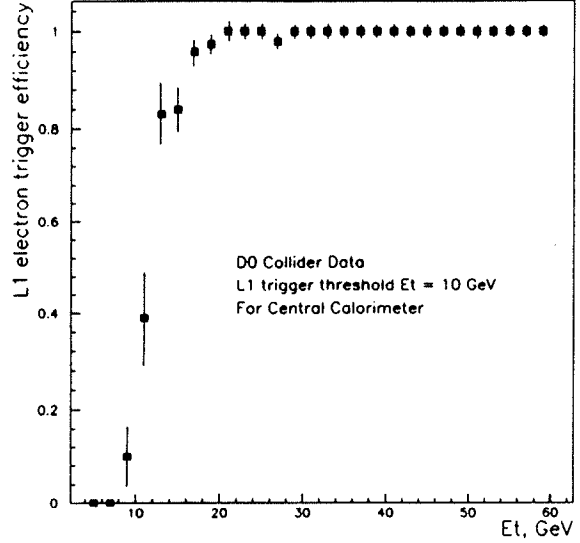


Figure 3. Efficiency of the Level1 electron triggers vs E_t of electrons.

The EC calorimeter response to electrons with energies from 10 to 150 GeV was studied in the 1990 run [1]. In 1991 the measurements were done for the Central calorimeter with electrons in an energy range from 2 to 150 GeV [3,4]. Using this data the energy resolution and linearity of the calorimeters were extracted. For both EC and CC the electromagnetic sampling resolution was roughly $15\%/\sqrt{E}$ with a constant term of 0.5%. The hadronic sampling resolution was found to be $50\%/\sqrt{E}$ with a constant term of 4%. The linearity of the calorimeter response is shown in Fig. 2. For electrons above 15 GeV it is linear within 0.3 %. For low energies a little loss in the response is seen. For electrons with an energy of 2.5 GeV the deviation from linearity is about 50 MeV [5].

The central tracking system consists of a vertex drift chamber (VTX), a transition radiation detector, a central drift chamber (CDC) and forward drift chambers (FDC). To identify electrons a track reconstructed in these chambers should match an electromagnetic cluster found in one of the D0 calorimeters. The position resolution of the central calorimeter extracted for test beam electrons is approximately $\delta dr = 3$ mm and $\delta dz = 3$ mm for high momentum electrons. While the position resolution of tracking chambers is much better, and for the CDC, for example, it is $\delta d\phi = 1$ mrad and $\delta d\theta = 10$ mrad.

3. TRIGGERS

The D0 trigger system for electrons consists of two levels of hardware triggers and one level of software triggers. Level0 selects a valid beam-beam crossing based on a scintillator coincidence. The Level1 triggers are used to find electron and jets candidates based on calorimeter information. The calorimeter processor covers $|\eta| < 4$. in trigger towers of $d\eta = 0.2$ by $d\phi = \pi/32$. Level 1 electron candidates are formed based on EM energy in

trigger towers exceeding one of several thresholds. 32 hardware triggers are defined as a logical combination of many hardware conditions. During the collider run seven D0 triggers included electrons.

The software filtering of events (Level 2 trigger) is performed on one of the 50 VAX 4000/60 nodes where the FORTRAN filtering code was running. For each hardware trigger bit there is a set of "filter tools". Software filter tools refine the hardware trigger decision using the full detector information. Filter tools exist for jets, muons, electrons, photons, missing E_t , scalar E_t and narrow jets. The electron and photon filtering tools make cuts on longitudinal shape (energy fractions in the four EM layers and in the first hadronic layer) and on the transverse shower shape using the 0.05×0.05 segmentation of the third EM layer. Many electron filters require the electron to be isolated in the calorimeter. In addition, track matching can be done for the electrons and that is the only difference between electrons and photons on that level. The Level 2 electron trigger with no track match and with a threshold of 20 GeV has a rejection factor of 25. A factor of 2 - 4 results from the track match requirement for $|\eta| < 1.2$ [6].

Both the hardware and software trigger performance are well reproduced by Monte Carlo simulations. The efficiency of the Level 1 triggers for isolated electrons vs E_t is shown in Fig.3. It is seen that for electrons with $E_t > 20$ GeV the efficiency of Level 1 is always better than 98%. The efficiency of the Level2 tools for W and Z electrons are better than 98%.

The first D0 collider run was devoted to high p_t physics and all electron triggers had high energy thresholds in Level1 ($E \geq 7$ GeV) and in Level2 ($E \geq 12$ GeV). However, some attempts have been made to reduce the trigger threshold down to 2.5 GeV to select $\Gamma \rightarrow e^+ + e^-$ and $J/\psi \rightarrow e^+ + e^-$ [7] decays and to study the D0 capabilities of doing B-physics with electrons. Two triggers were tested. The first trigger was used to collect a sample of events with two electrons and an associated "jet". That trigger required the presence of two trigger towers with EM energy exceeding 2.5 GeV, while the energy deposit in the hadronic layers had to be smaller than 1 GeV and required a jet with $p_t > 2.5$ GeV. The other trigger did not require a jet and was prescaled by a factor of 3. The Level1 rates for those triggers were measured at a luminosity of $2.8 \times 10^{30} \text{ cm}^{-2} \text{ sec}^{-1}$ as 60 Hz and 90 Hz respectively. This means that with certain modifications such triggers can be included in the D0 trigger list. The Level2 tools apply shape cuts and isolation cuts which were tuned on isolated electrons from test beam data down to 5 GeV. In addition to them several filters with loose isolation cuts were introduced to record non-isolated electrons. At the moment intensive Monte Carlo and off-line studies are being conducted to analyse the obtained data and estimate rejection factors and efficiencies.

4. OFF-LINE ALGORITHMS

The off-line electron ID technique is based on the fact that the shape of the electromagnetic and hadronic showers can be used to differentiate between electrons (photons) and hadrons. Electrons deposit almost all their energy in the EM section of the calorimeter, while hadrons deposit significant amounts of energy in the hadronic layers. The cut on the fraction of the energy in the EM calorimeter ($f_{EM} > 90\%$) has an efficiency of greater than 99% for the test beam electrons with energy 10 - 150 GeV.

To improve the discrimination against hadrons both the longitudinal and the transverse shower shape should be taken into account. That may be done using an H-matrix technique [1,8,9]. For a "training" sample of Monte Carlo generated electron showers us-

ing the mean energy $\langle E_i \rangle$ deposited in a calorimeter cell, one can define the correlation coefficient C_{ij} , as

$$C_{ij} = \langle (E_i - \langle E_i \rangle)(E_j - \langle E_j \rangle) \rangle.$$

The covariance H-matrix then is:

$$H_{ij} = C_{ij}^{-1}.$$

For each event an effective χ^2 is calculated from:

$$\chi^2 = \sum_{i,j} (E_i - \langle E_i \rangle) H_{ij} (E_j - \langle E_j \rangle).$$

The D0 calorimeter has finer transverse segmentation in the third EM layer. In addition to the fraction of shower energy in the first EM layer (EM1), the fraction of shower energy in the second EM layer (EM2) and in the fourth EM layer (EM4) we included in the H matrix definition the fraction of shower energy in each cell of a 6×6 array centered on the hottest tower in the third EM layer. To include the energy and impact parameter dependence into the matrix the logarithm of the total energy and the position of the event vertex were added as parameters. This gives us a 41 dimensional matrix. To simulate the electron shower we used GEANT 3.14 and a detailed representation of the calorimeter geometry. We have verified the excellent agreement of the MC with the calorimeter response and then trained the H-matrix for each of the 37 different detector η towers. Using this H-matrix for the collider events we are able to calculate a χ^2 and place a cut to separate EM and Hadronic showers.

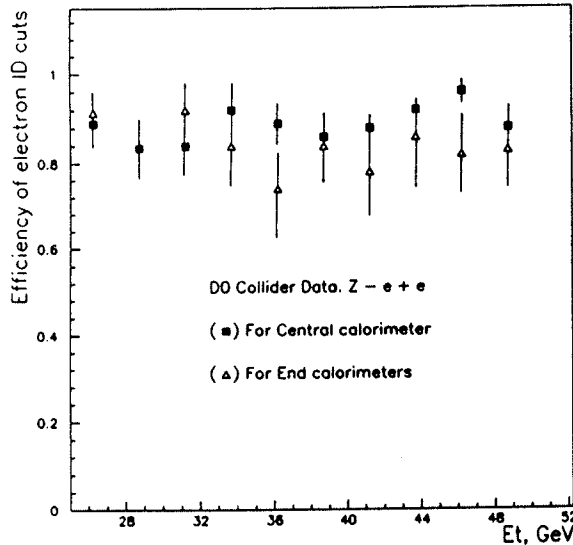


Figure 4. Efficiency of the standard D0 electron ID cuts for $Z \rightarrow e^+ + e^-$ events.

The electron identification is done in three steps. First of all electron candidates are identified as nearest neighbor clusters of the EM and the first hadronic layer calorimeter cells. Then the fraction of the energy deposited in EM layers is calculated for the cells forming the cluster. For the clusters which pass the cut on the fraction of EM energy we calculate the H-matrix χ^2 and find a track matched with the position in the calorimeter. We define the position of the shower centroid using a weighted center of gravity method [10]. In Fig.4 the efficiency of the standard electron ID cuts [11] is shown for $Z \rightarrow e^+ + e^-$. It is seen that the efficiency is about 80% with no systematic dependence on the electron E_t .

5. ELECTRON/PION DISCRIMINATION

To obtain the best discrimination against hadrons and to provide high electron finding efficiency the H-matrix χ^2 cuts were carefully selected. The H-matrix was applied to test beam electrons and the χ^2 cut was chosen to have 95% efficiency. Then the pion rejection factor was determined by applying the same cuts to single pion test beam data. The rejection factors are shown in Fig. 5 as a function of pion momentum for the case of cutting $HAD/EM < 0.02$ ($f_{EM} > 98\%$), and for the case of a cut on $HAD/EM < 0.04$ ($f_{EM} > 96\%$) followed by the H-matrix χ^2 cut. It is seen that the rejection factor is 900-3000 for particles with momentum 50 - 150 GeV/c.

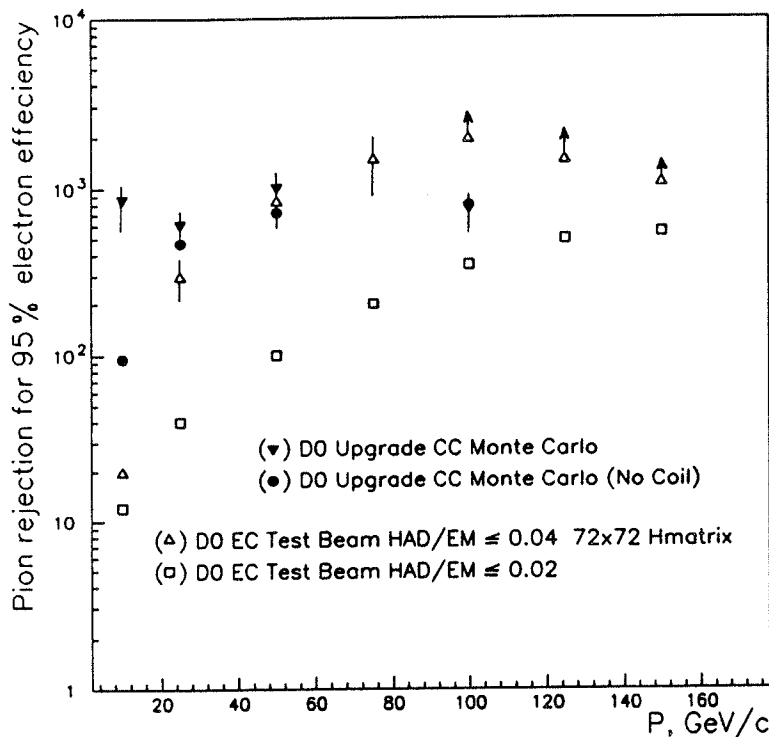


Figure 5. Pion/electron rejection factor vs pion momentum.

For energies below 20 GeV the situation becomes worse and the rejection factor does not exceed 10. As it was shown in [12], for the fully upgraded D0 detector it is possible using a modified H-matrix to obtain larger pion rejection factors for energies below 50 GeV. After the full upgrade the current D0 tracking system will be replaced by a combination of silicon microstrip barrel and disk detectors along with a full scintillating fiber tracker. These detectors will be located inside a superconducting solenoid, with a preshower detector located just outside the magnet. For the electron ID studies an H-matrix was generated using additional information from the preshower detector and the position of the interaction vertices. Using the Monte Carlo generated H-matrix plus the E/p cut and calorimeter/preshower position matching, electron/pion rejection factors were calculated. In Fig.5 solid points and triangles represent these calculations. It can be seen that the predicted rejection factor is more than 500 for all energies starting from 10 GeV. The main improvement observed in pion rejection at low energy is due to the E/p cut.

6. MODIFICATION OF ELECTRON ID FOR B-PHYSICS

The electron ID techniques discussed above were created for isolated high energy electrons. For B-physics studies where low energy electrons are often accompanied by hadrons the efficiency of electron finding dropped down to 30% [12] after applying the cuts tuned for isolated particles. This makes especially important the optimization of isolation criteria for both Level 2 triggers and off-line algorithms. It also means that transverse shower development parameters included in the H-matrix should be much more carefully selected assuming the possible presence of hadrons near electrons. One of the solutions here may be using the H-matrix with only longitudinal shower development parameters, loose isolation cuts together with tight track matching requirements. Using the obtained data and MC generated events the electron ID algorithms for low-energy non-isolated electrons are now being tested. These studies should be performed together with necessary trigger simulations before the coming collider run (1b) when we hope to include electron triggers for B-events.

7. REFERENCES

1. S. Abachi et al., *Nucl. Instr. Meth.* **A324**(1993)53.
2. H. Aihara et al., to be published in *Nucl. Instr. and Meth. A*.
3. P. Bhat, *Proceedings of the American Physical Society Division of Particles and Fields Conference, Fermilab*, Nov, 1992.
4. K. De, *Proceedings of the XXVI International Conference on High Energy Physics*, Aug, 1992, Dallas, Texas.
5. N. Denisenko, *Internal D0 Note 1852*, Aug, 1993.
6. J. Linnemann, *Proceedings of the American Physical Society Division of Particles and Fields Conference, Fermilab*, Nov, 1992.
7. M. Tartaglia, *Internal D0 Note 1723*, May, 1993.
8. R. Engelmann et al., *Nucl. Instr. Meth.* **216**(1983)45.
9. M. Narain, *Proceedings of the American Physical Society Division of Particles and Fields Conference, Fermilab*, Nov, 1992.
10. T.C. Awes et al., *Nucl. Instr. Meth.* **A311**(1992)130.
11. U. Heintz, M. Narain, *Internal D0 Note 1814*, Jul, 1993.
12. S. Abachi et al., *Internal D0 Note 1733*, May, 1993.

